IOPscience iopscience.iop.org

Home Search Collections Journals About Contact us My IOPscience

Large-scale synthesis of copper nanoparticles by chemically controlled reduction for applications of inkjet-printed electronics

This article has been downloaded from IOPscience. Please scroll down to see the full text article.

2008 Nanotechnology 19 415604

(http://iopscience.iop.org/0957-4484/19/41/415604)

View the table of contents for this issue, or go to the journal homepage for more

Download details:
IP Address: 132.205.8.118
The article was downloaded on 17/09/2013 at 17:28

Please note that terms and conditions apply.

Nanotechnology **19** (2008) 415604 (7pp) doi:10.1088/0957-4484/19/41/415604

Large-scale synthesis of copper nanoparticles by chemically controlled reduction for applications of inkjet-printed electronics

Youngil Lee, Jun-rak Choi, Kwi Jong Lee, Nathan E Stott and Donghoon Kim

Samsung Electro-Mechanics, Central R&D Institute, Electro-Materials and Devices (eMD) Center, Functional Materials Technology Group, Nanomaterials Team, 314 Maetan-3-Dong Yeongtong-Gu, Suwon, Gyeonggi-Do 443-743, Korea

E-mail: youngil1.lee@samsung.com

Received 22 March 2008, in final form 3 July 2008
Published 4 September 2008
Online at stacks.iop.org/Nano/19/415604

Abstract
Copper nanoparticles are being given considerable attention as of late due to their interesting properties and potential applications in many areas of industry. One such exploitable use is as the major constituent of conductive inks and pastes used for printing various electronic components. In this study, copper nanoparticles were synthesized through a relatively large-scale (5 l), high-throughput (0.2 M) process. This facile method occurs through the chemical reduction of copper sulfate with sodium hypophosphite in ethylene glycol within the presence of a polymer surfactant (PVP), which was included to prevent aggregation and give dispersion stability to the resulting colloidal nanoparticles. Reaction yields were determined to be quantitative while particle dispersion yields were between 68 and 73%. The size of the copper nanoparticles could be controlled between 30 and 65 nm by varying the reaction time, reaction temperature, and relative ratio of copper sulfate to the surfactant. Field emission scanning electron microscopy (FE-SEM) and transmission electron microscopy (TEM) images of the particles revealed a spherical shape within the reported size regime, and x-ray analysis confirmed the formation of face-centered cubic (FCC) metallic copper. Furthermore, inkjet printing nanocopper inks prepared from the polymer-stabilized copper nanoparticles onto polyimide substrates resulted in metallic copper traces with low electrical resistivities ($\geqslant$3.6 $\mu\Omega$ cm, or $\geqslant$2.2 times the resistivity of bulk copper) after a relatively low-temperature sintering process (200 °C for up to 60 min).

1. Introduction

With increasing demands for more economic routes to the manufacture of electronic devices incorporating polymer-based printed circuit boards (PCBs), various techniques for the fabrication of microelectronic devices, including screen printing, nano-imprinting, inkjet printing, and direct printing, are generating increasing interest. Among these methods, inkjet printing is considered to be an economical and highly functional technology for the microscale patterning of metallic traces in microelectronic devices. Thus, many research efforts are currently being devoted to develop the inkjet printing method as a patterning tool that will substitute traditional photolithography methods used for making micron-sized patterns [1]. Conventional lithographic processes are well developed but include multiple steps that are time consuming, uneconomical, and not versatile towards corrective repatterning [2, 3]. However, the employment of inkjet printing can solve many of the problems in a facile and effective manner. The inkjet printing method allows for the patterning of conductive traces onto a substrate in one step, therefore reducing the time, cost, and space consumed and the toxic

 © 2008 IOP Publishing Ltd Printed in the UK

waste created during the manufacturing process [1, 4–6]. The fully data driven and maskless nature of drop on demand (DOD) inkjet processing allows more versatility than other direct printing methods, such as easily allowing corrective overprinting. Inkjet printing is an additive method in which materials dispersed in a carrier solution are deposited onto a given substrate by piezo-electrically driven micro-nozzles. Such a solution processing-based method provides enhanced flexibility for choosing both the deposition material and the substrate [7].

Nanomaterials are considered to be highly useful for application of materials through inkjet printing technology based on size-dependent mesoscopic properties such as enhanced dispersibility, melting point depression below that of the same bulk material based on more significant surface energy instability, and greater compatibility with various chemical and physical environments due more significant effects from interchangeable surface coatings. Inkjet printing technology employing conductive silver inks has been developed recently in order to manufacture low-cost disposable electronics, such as smart packaging, RF-ID tags, and digital calendars. Various silver inks based on organosilver compounds and silver nanoparticle suspensions have been used for inkjet printing conductive traces [8–10]. However, silver as a conductive material has problems due to ion migration at relatively high-temperature and humidity conditions as well as cost-benefit issues compared to copper, which is significantly less expensive for virtually identical bulk conductivities. Thus, copper-based nanoparticle inks are being considered as a preferable material for microscale patterning. However, some disadvantages of copper which must be overcome are that the copper ion is not easily reduced under mild reaction conditions and copper nanoparticles tend to be easily oxidized in air under ambient atmospheric conditions in comparison to noble metals like gold and silver.

Many schemes reported in the literature have been developed for the preparation of copper particles, such as thermal decomposition, microemulsions, UV irradiation, reduction of aqueous copper salts, and the polyol process [11–15]. However, most of the synthetic methods are not economically feasible due to low throughput (<0.1 M) and poor scalability. Furthermore, the sizes of copper particles produced from many of these methods are in the submicron to micron regimes, resulting in lower dispersion stabilities and higher melting points. Thus, in order to reap the economic benefits of inkjet-printed electronics, economically feasible processes to produce nanomaterials must be developed to overcome the low-concentration conditions typical for nanoparticle formation and lack of scalability due to temperature and mixing gradients in batch processes. Additionally, inkjet-printed materials must be processable into high-performance electronic components at low enough temperatures to yield additional economic benefits through allowing the use of inexpensive plastic substrates that tend to warp and melt at higher processing temperatures.

In this research, a large-scale (5 l), high-throughput (0.2 M) process for the synthesis of copper nanoparticles was developed using a modified polyol process that includes chemical reduction and hot addition. Furthermore, these copper nanoparticles were dispersed into an ether-based solvent, patterned onto various substrates through inkjet printing, and then converted into conductive metallic traces through a relatively low-temperature, reductive sintering process.

2. Experimental details

2.1. Materials and synthesis

Polyvinylpyrrolidone (PVP, K-30), sodium hypophosphite monohydrate ($NaH_2PO_2 \cdot H_2O$), copper sulfate pentahydrate ($CuSO_4 \cdot 5H_2O$), ethylene glycol, acetone, and 2-(2-butoxy-ethoxy)ethanol were all analytical grade and used without further purification.

Copper nanoparticles were synthesized by the following procedure: 1.11 kg PVP and 400 g sodium hypophosphite were mixed into 4 l ethylene glycol inside a round-bottom flask while vigorously stirring at room temperature under ambient atmosphere. The mixture was heated to 90 °C at a rate of 5 °C min^{-1}. Then, 1 l of a 1 M solution of copper sulfate in ethylene glycol at 90 °C was rapidly added into the PVP/sodium hypophosphite solution while stirring vigorously. As reduction occurred, the color of the suspension turned from green to henna within 2–3 min, indicating the formation of copper nanoparticles. The reaction was quenched and the suspension was rapidly cooled by adding chilled deionized (DI) water. The copper nanoparticles were separated and washed with DI water by centrifugation, while using acetone as a non-solvent, in order to remove excess PVP and side products. The resulting precipitates were dried under vacuum at 40 °C for 2–3 h.

Reaction yields were determined through gravimetric analysis of isolated, vacuum-dried samples where the contributions of surface organics and volatiles based on TGA data were removed. Dispersion yields were determined by the following procedure. A known weight of copper nanoparticles was dispersed into ethanol at 20% by weight through shear mixing for 15 min followed by microfluidization. The resulting dispersion was centrifuged at 3000 rpm for 3 min. The supernatant was decanted and the resulting sediment was dried in a vacuum oven to completeness. Finally, the dispersion yield was determined from the known starting weight of copper and the weight of sediment found by gravimetric analysis. The copper nanoparticles that remained dispersed in the ethanol supernatant were isolated and then used for ink production.

2.2. Inkjet printing and reductive sintering

Conductive inks at 30% weight of copper were prepared from dispersible copper nanoparticles by shear mixing into 2-(2-butoxyethoxy)ethanol for 15 min followed by microfluidization. The resulting nanocopper inks were pressed through 0.4 μm syringe filters to eliminate any large particles, aggregates, and agglomerates. Conductive traces were printed onto various substrates using an iTi industrial inkjet printing system equipped with a Dimatix Spectra SE piezoelectric print head that has 128 nozzles of 38 μm diameter. The distance

between the nozzles and the substrate was 500 mm. While a common problem with particles that have poor dispersive properties in inks, clogging of the print head nozzles did not occur during these experiments. The substrate temperature was maintained at 85 °C to cause the ink to cure more quickly. After printing at a resolution of 500 dpi, the copper ink patterns were cured and sintered at 200 °C for 1 h in a tube furnace under reductive atmosphere (nitrogen gas bubbled through formic acid) to reverse and prevent oxidation.

2.3. Characterization

The size and shape of the copper nanoparticles were determined using field emission scanning electron microscopy (FE-SEM, S-4700, Hitachi, Japan) and transmission electron microscopy (TEM, JEM 2000FXII, JEOL, Japan) with an accelerating voltage of 200 kV. The crystal structure of the copper nanoparticles was identified using x-ray diffractometry (XRD, D/max-2500, Rigaku, Japan) operated at 40 kV and 150 mA with Cu Kα radiation and confirmed by selected area electron diffraction (SAED) performed during TEM imaging. The size distributions of copper nanoparticles were determined through dynamic light scattering (DLS, Nanotrac NPA 252, Microtrac, USA), and the average particle sizes were calculated from XRD patterns according the Scherrer equation:

$$L = \frac{K\lambda}{\beta \cos\theta}$$

where L is the average particle size, K is the Scherrer constant related to the shape and index (hkl) of the crystals, λ is the wavelength (1.7889 Å) of the x-rays, β is the additional broadening (in radians), and θ is the Bragg angle. The content of organics on the surfaces and oxidation onset temperature for the copper nanoparticles were determined by performing thermo-gravimetric analysis (TGA, SDT Q600, TA Instruments, USA) in both nitrogen and air with a heating rate of 10 °C min^{-1} from room temperature to 600 °C. Viscosities were measured by rheometry (DV-III+, spindle #18, Brookfield, USA), and surface tensions were measured by tensiometry (K10ST, Krüss, Germany) for the copper inks in which the measuring temperature was maintained at 25 °C by a temperature-controlled circulator. The specific electrical resistance (resistivity) was calculated from four-point probe resistance and optical profilometry (VK-9510K 3-D Profile Microscope, Keyence, Japan) measurements with the equation

$$\rho = \frac{RA}{\ell}$$

where ρ is the resistivity, R is the electrical resistance, A is the cross-sectional area (film thickness), and ℓ is the length.

3. Results and discussion

3.1. Synthesis of copper nanoparticles

The mechanism of metal reduction by hypophosphite ions has been described by various schemes [16]. Some authors have proposed that the metal ions are reduced by atomic hydrogen evolving from the reaction of hypophosphite with water:

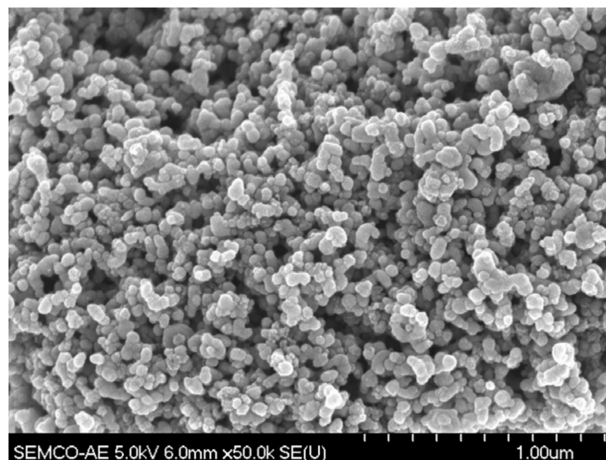

Figure 1. FE-SEM image of copper nanoparticles. The sample was prepared from an ethanol dispersion dropcast and dried into a thin film on a PI substrate, followed by sputter coating a thin layer of platinum for added contrast.

$$H_2PO_2^- + H_2O \rightarrow H_2PO_3^- + 2H. \quad (1)$$

In this case, the total reduction process may be written as follows:

$$M^{2+} + H_2PO_2^- + H_2O \rightarrow M^0 + H_2PO_3^- + 2H^+. \quad (2)$$

Evolution of gaseous hydrogen is explained by recombination of atomic hydrogen:

$$2H \rightarrow H_2. \quad (3)$$

However, it has been experimentally established that the reduction of one M^{2+} cation corresponds to oxidation of two hypophosphite anions according to the equation

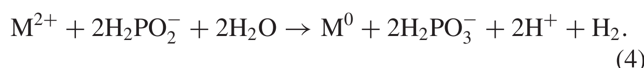

$$M^{2+} + 2H_2PO_2^- + 2H_2O \rightarrow M^0 + 2H_2PO_3^- + 2H^+ + H_2. \quad (4)$$

Color changes during the course of the reaction indicate the formation of different complexes between copper sulfate and hypophosphite. As the copper sulfate solution is introduced into the hypophosphite solution, the blue copper sulfate solution becomes colorless (stage I), then turns green (stage II), and finally turns henna (stage III). The intermediate steps of the reduction mechanism for the synthesis are described as follows.

Stage I—formation of colorless copper(II) complex:

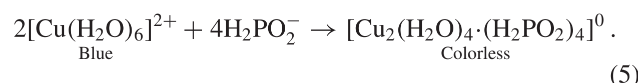

$$\underset{\text{Blue}}{2[Cu(H_2O)_6]^{2+}} + 4H_2PO_2^- \rightarrow \underset{\text{Colorless}}{[Cu_2(H_2O)_4 \cdot (H_2PO_2)_4]^0}. \quad (5)$$

The neutral complex may be either mononuclear or dinuclear. The probability of forming the dinuclear complex is higher for higher reactant concentrations.

Stage II—reduction of copper(II) to copper(I) with concomitant formation of green copper(I) complex:

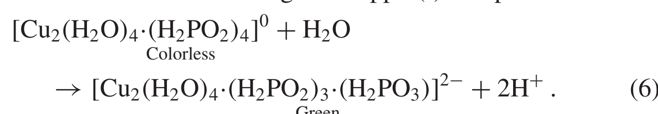

$$\underset{\text{Colorless}}{[Cu_2(H_2O)_4 \cdot (H_2PO_2)_4]^0} + H_2O \rightarrow \underset{\text{Green}}{[Cu_2(H_2O)_4 \cdot (H_2PO_2)_3 \cdot (H_2PO_3)]^{2-}} + 2H^+. \quad (6)$$

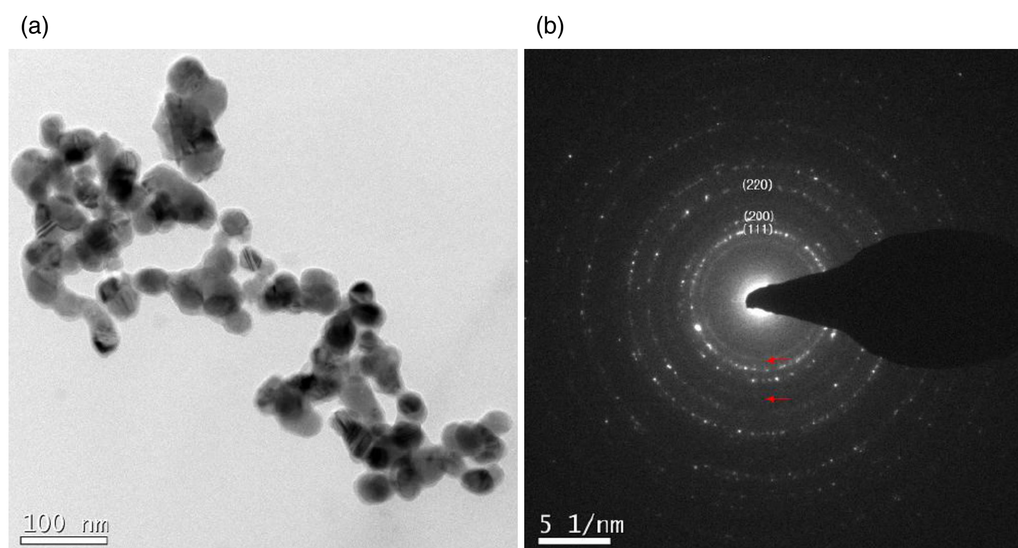

Figure 2. (a) TEM image and (b) corresponding SAED pattern of the copper nanoparticles obtained under optimum synthetic conditions.

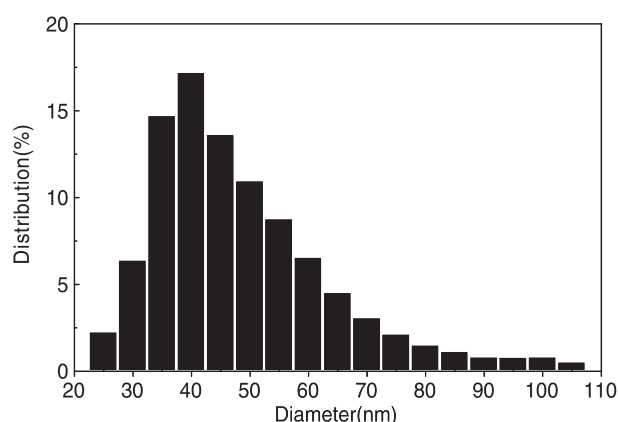

Figure 3. DLS of as-prepared copper nanoparticles without size selection.

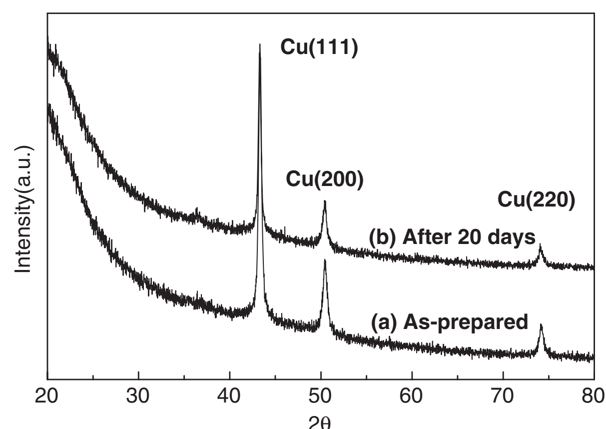

Figure 4. X-ray diffraction patterns of isolated copper nanoparticles (a) soon after and (b) 20 days after preparation.

The resulting green color is a typical characteristic of copper(I) salt solutions. Stage III results from further reduction to yield highly dispersed metallic copper, causing the solution to turn henna in color.

Stage III—reduction of copper(I) to dispersed copper(0):

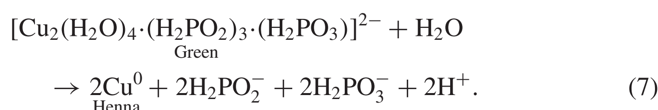

$$\underset{\text{Green}}{[Cu_2(H_2O)_4{\cdot}(H_2PO_2)_3{\cdot}(H_2PO_3)]^{2-}} + H_2O \rightarrow \underset{\text{Henna}}{2Cu^0} + 2H_2PO_2^- + 2H_2PO_3^- + 2H^+. \quad (7)$$

By combining reaction equations (5)–(7), the following equation is obtained:

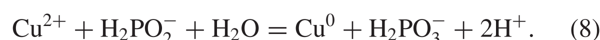

$$Cu^{2+} + H_2PO_2^- + H_2O = Cu^0 + H_2PO_3^- + 2H^+. \quad (8)$$

From the combined equation, it can be seen that the consumption of hypophosphite anion is directly related to copper reduction.

As can be predicted based on equations (8) and Le Chatelier's Principle, an excess quantity of hypophosphite being introduced into the reaction system will cause the reduction rate of copper cation to become faster. However, in the case of extreme excesses of hypophosphite, the reaction system becomes unstable due to the sudden evolution of gaseous hydrogen that is generated. Thus, it is important that the synthesis be carried out at an optimum mole ratio of hypophosphite-to-copper precursor. Under the optimized conditions presented in this paper, the synthesis of copper nanoparticles results in virtually quantitative reaction yields as found from a combination of recovery data generated by gravimetric analysis and TGA.

The polyol in the polyol process acts as both a solvent and reducing agent. Additionally, the polyol stabilizes the surfaces of the particles to help prevent agglomeration and the uncontrolled growth of particles [17, 18]. Thus, the polyol helps facilitate the growth of smaller particles in more narrow size regimes. However, the reaction rate of the polyol process is relatively slow, often requiring the reaction solution to be held under refluxing conditions for much longer times. In aqueous chemical reductions used to prepare copper

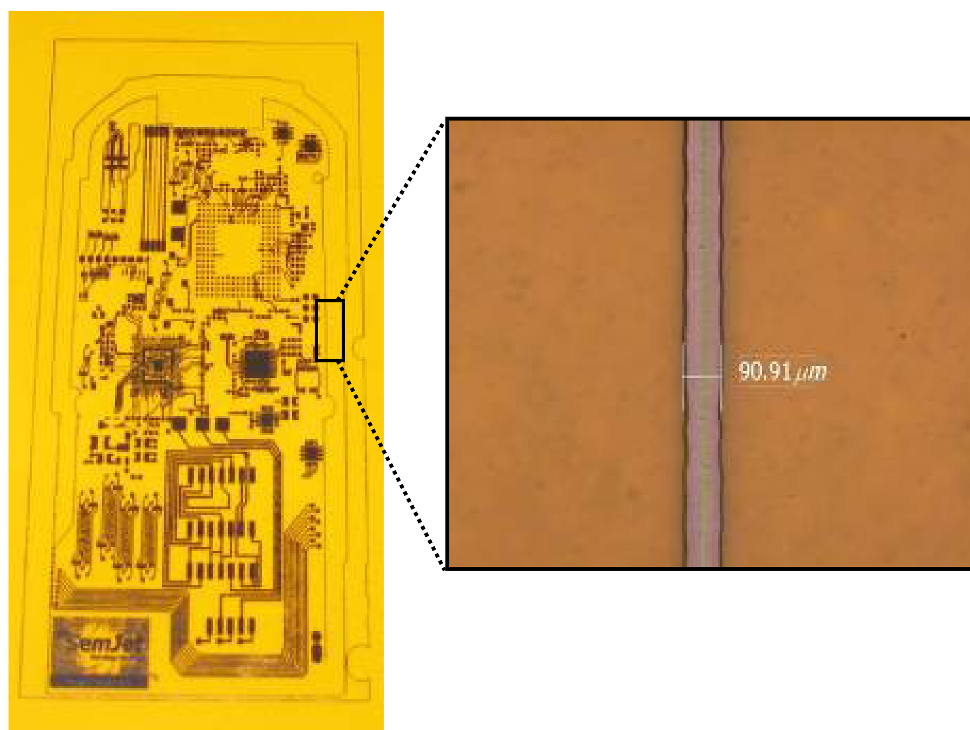

Figure 5. Conductive copper pattern inkjetted onto polyimide substrate. (This figure is in colour only in the electronic version)

particles, sodium hypophosphite is commonly employed as a reducing agent, the reaction rate of systems being very fast due to the strong complexation of hypophosphite-to-copper ions. However, the agglomeration of particles in such schemes is often severe [19]. The synthetic procedure introduced in this study has several important advantages over conventional polyol and aqueous preparation methods by combining the quick, low-temperature reducing powers of sodium hypophosphite with the enhanced stability of polyol solvent. Furthermore, copper nanoparticles with improved size and uniformity are obtained by exploitation of the hot addition technique. Finally, this single synthetic process to produce well-dispersed copper nanoparticles at 47–50 gram scale quantities provides additional means of control through modifying the reducing agent-to-copper precursor mole ratio along with reaction conditions, such as temperature and time.

The dispersion stability of the nanoparticles is a key property with respect to inkjet printing performance. Even the most monodisperse nanoparticles of an ideal size are useless for inkjet applications in the case of poor dispersion stability. One of the additional strengths of the synthesis presented in this work is the relatively high dispersion stability of the resulting nanoparticles, which were typically between 68 and 73%. Dispersible copper nanoparticles in 2-(2-butoxyethoxy)ethanol inks were stable for more than three weeks in a stationary state without any significant additional sedimentation. Two factors may contribute to this enhanced dispersion stability. First, the smaller sizes of copper nanoparticles reported in this work compared to others in the literature that are in the lower submicron size regime and contain more significant amounts of copper nanoparticle agglomerates and aggregates [20]. Second, the addition of PVP as a surfactant polymer that coats the nanoparticle surfaces. In many metal nanoparticle preparations, PVP is typically added as a protective surface coating that controls the growth during the reaction, prevents aggregation through steric hindrance during and after the reaction, and interacts with polar solvents to aid in dispersing the nanoparticles.

3.2. Size and shape analyses

Copper nanoparticles separated from the henna-colored suspension were analyzed for their size distribution and shape by FE-SEM, TEM, and DLS, along with a comparison to average sizes calculated from XRD peak data. Figure 1 shows an FE-SEM image of copper nanoparticles as prepared by the reported process, revealing spherically shaped particles with some agglomeration and aggregation. Figure 2 depicts a TEM image and the corresponding selected area electron diffraction (SAED) pattern of the as-prepared product. This image also shows that the product consists of spherical primary particles, and the diffraction pattern yields further confirmation of an FCC structure. Figure 3 depicts the size distribution based on DLS data, revealing that most of the distribution falls between 30 and 65 nm in diameter, with a number-weighed mean of 55 nm.

3.3. Crystallographic characteristics

XRD patterns of the copper nanoparticles prepared for this work are displayed in figure 4 with 2θ values between

20° and 90°. The XRD pattern in figure 4(a) shows three characteristic peaks at 44.6°, 51.8°, and 76.2° for the respectively marked indices of (111), (200), and (220). These characteristic peaks confirm the formation of a face-centered cubic (FCC) copper phase without significant oxides or other impurity phases. Generally, nanoscale particles are metastable owing to higher percentages of surface area, causing them to be more readily oxidized in air. However, the copper nanoparticles in this work show a significantly oxide-free, stable FCC copper phase even after 20 days of storage in a vial under ambient conditions (figure 4(b)). The average primary particle size of the copper nanoparticles was calculated from the full width at half maximum (FWHM) of the (111) peaks in the XRD patterns using the Scherrer equation, resulting in an average primary particle size of about 32 nm. Comparison of the average particle size calculated using the Scherrer equation with the particle sizes determined from DLS (figure 3) and the sizes and shapes visible in SEM images (figure 1) led to the conclusion that particles at the larger side of the distribution are agglomerates that skew the number-weighed mean size to be greater than the average primary particle size calculated from XRD data[1].

3.4. Ink preparation, rheological properties, and inkjet printing

Nanocopper ink was prepared by dispersing the dispersible copper nanoparticles into 2-(2-butoxyethoxy)ethanol through shear mixing and microfluidization. The copper ink in this study had a measured viscosity of 12.3 cP and surface tension of 29 $\mathrm{N\,m^{-1}}$ at metallic copper concentrations of 30% by weight. The dispersed copper nanoparticles could be suspended for several weeks in the stationary state and more than 3 min under centrifugation at 3000 rpm without further sedimentation. Figure 5 shows metallic copper traces that were printed onto a polyimide substrate using a Spectra SE head, under an optimized waveform, and then sintered at 200 °C for 1 h under a reducing atmosphere. This print test thus confirms that fine patterning for microelectronics is possible when employing nanocopper inks generated from this process.

3.5. Thermal and electrical properties

TGA results of the polymer-stabilized copper nanoparticles obtained under optimum chemical conditions are shown in figure 6. Under a nitrogen atmosphere, sharp weight losses occur from 50 to 170 °C and from 220 to 350 °C, as shown in figure 6(a). These are related to the drying of residual washing solvent and decomposition of polymer surface coatings respectively. The resulting organics and volatiles content is approximately 7.4% by weight. Under air, a weight gain of about 20% due to the oxidation of copper has an onset at about 180 °C before stopping at about 600 °C in figure 6(b). This means that the copper nanoparticles begin to thermally oxidize at about 180 °C and higher to form copper oxide. Thus, the sintering process of copper nanoparticles must be performed under a reducing atmosphere to avoid oxidation.

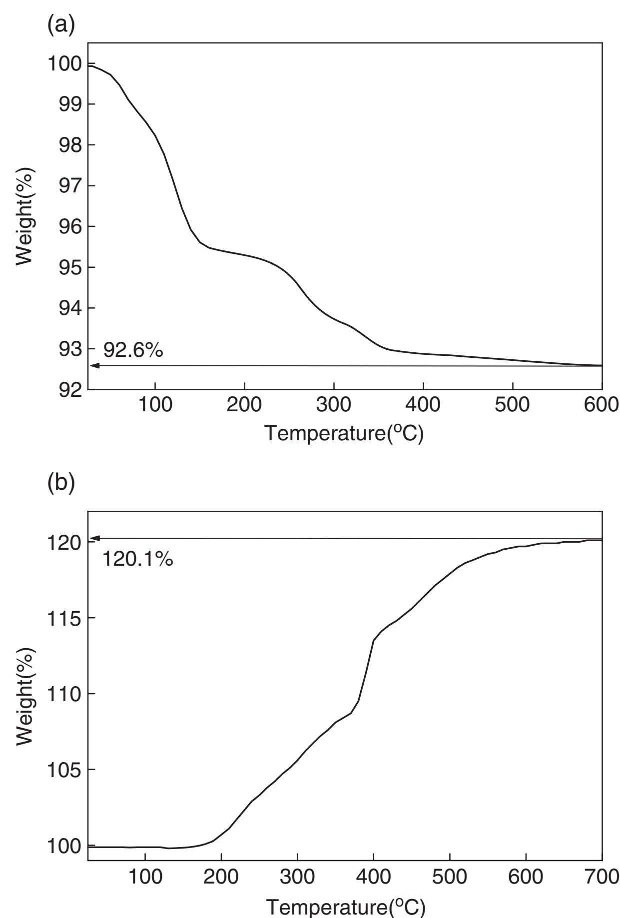

Figure 6. TGA curves of copper nanoparticles obtained under (a) N_2 and (b) air.

The electrical resistivities of metallic copper patterns on polyimide as a function of sintering time at 200 °C under a reducing gas flow are exhibited in figure 7. The resistivities decreased from 45 $\mu\Omega$ cm after 20 min to 3.6 $\mu\Omega$ cm, or 2.2 times the resistivity of bulk copper, after 60 min of sintering time. This shows that the electrical resistivity is sufficiently low to behave as an electrical conductor, even though the copper nanoparticles were sintered at a relatively low temperature. Such low-temperature sintering conditions resulting in relatively low resistivities make nanocopper inks produced from this process ideal for use on inexpensive, thermally unstable plastic substrates that require lower processing temperatures to avoid warping.

4. Conclusion

Copper nanoparticles within a more preferable size regime have been successfully prepared at higher concentrations by a modified polyol process using sodium hypophosphite as

[1] These results are such since DLS data are generated from the scattering of the entire volume such that agglomerates are not readily distinguishable from single primary particles whereas peak narrowing for a given crystal face generated in the XRD data results from the volume of crystalline material in the primary particles without contributions from the amorphous polymer coatings. However, this explanation does involve some simplification due to the facts that different materials scatter light differently in the case of DLS and that a broad peak from amorphous solids must be subtracted from the baseline in the case of XRD.

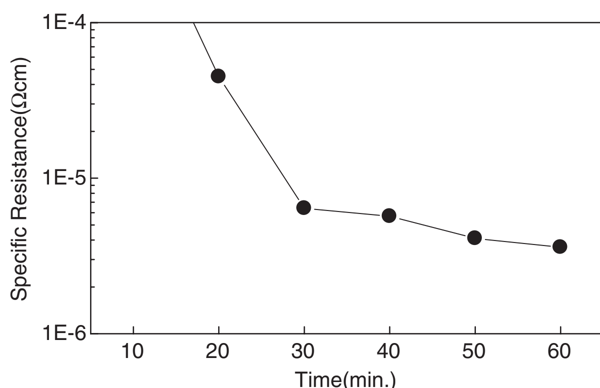

Figure 7. Resistivity of copper pattern on a polyimide substrate as a function of time sintered at 200 °C under a reducing atmosphere.

a reducing agent and PVP as a stabilizing polymer. The resulting copper nanoparticles did not experience significant oxidation even after 20 days under ambient storage conditions. Furthermore, these copper nanoparticles displayed excellent dispersion yields and dispersion stabilities of dispersed particles without additional sedimentation. The hot addition technique and controlling of the reducing agent-to-copper precursor mole ratio used in this study are considered to have played important roles in the resulting formation of smaller and well-dispersed copper nanoparticles. The resistivity of the resulting copper pattern was low even given the low sintering temperature. Based on the inkjet printability test in this study, copper nanoparticles synthesized by the method presented in this work can be considered a highly useful material for microscale patterning.

References

[1] Calvert P 2001 *Chem. Mater.* **13** 3299
[2] Arias A C *et al* 2004 *Appl. Phys. Lett.* **85** 3304
[3] Sabnis R W 1999 *Displays* **20** 119
[4] Fuller S B, Wilhelm E J and Jacobson J M 2002 *J. Microelectromech. Syst.* **11** 54
[5] Sirringhaus H, Kawase T, Friend R H, Shimida T, Inbasekaran M, Wu W and Woo E P 2000 *Science* **290** 2123
[6] Hong C M and Wagner S 2000 *IEEE Electron Device Lett.* **21** 384
[7] Ko S H, Chung J, Pan H, Grigoropoulos C P and Poulikakos D 2007 *Sensors Actuators* A **134** 161
[8] Peng W, Hurskainen V, Hashizume K, Dunford S, Quander S and Vatanparast R 2005 *IEEE Electronic Components and Technology Conf.* vol 77
[9] Szezech J B, Megaridis C M, Gamota D R and Zhang J 2000 *IEEE Trans. Electron. Packag. Manuf.* **25** 26
[10] Ryu B H, Choi Y, Park H S, Byun J H, Kong K, Lee J O and Chang H 2005 *Colloids Surf.* A **270/271** 345
[11] Aslam M, Gopakumar G, Shoba T L, Mulla I S, Vijayamohanan K, Kulkarni S K, Urban J and Vogel W 2002 *J. Colloid Interface Sci.* **255** 79
[12] Qi L M, Ma J M and Shen J L 1997 *J. Colloid Interface Sci.* **186** 498
[13] Kapoor S, Palit D K and Mukherjee T 2002 *Chem. Phys. Lett.* **355** 383
[14] Figlarz M, Fievet F and Kagier J P 1998 *US Patent Specification* 5759230
[15] Kuriahra L K, Chow G M and Schoen P E 1995 *Nanostruct. Mater.* **5** 607
[16] Chernogorenko V B and Tasybaeva Sh T 1995 *Russ. J. Appl. Chem.* **68** 461
[17] Goia C, Matijević E and Goia D V 2005 *J. Mater. Res.* **20** 1507
[18] Cai W and Wan J 2007 *J. Colloid Interface Sci.* **305** 366
[19] Liu Z J, Zhao B, Zhang Z T and Hu L M 1996 *Chin. Chem. Bull.* **10** 55
[20] Xuan Y and Li Q 2000 *Int. J. Heat Fluid Flow* **21** 58